

Evidence for an Intervening Stellar Population Toward the Large Magellanic Cloud¹

Dennis Zaritsky and D.N.C. Lin

UCO/Lick Observatory and Board of Astronomy and Astrophysics, Univ. of California at Santa Cruz,
Santa Cruz, CA 95064. Email: dennis@ucolick.org, lin@ucolick.org

¹ Lick Bulletin No. 1364

ABSTRACT

We identify a vertical extension of the red clump stars in the color magnitude diagram (CMD) of a section of the Large Magellanic Cloud (LMC). The distribution of stars in this extension is indistinguishable in the U , B , V , and I bands — confirming that the detection is real and placing a strong constraint on models of this stellar population. After subtracting the principal red clump component, we find a peak in the residual stellar distribution that is ~ 0.9 mag brighter than the peak of the principal red clump distribution. We consider and reject the following possible explanations for this population: inhomogeneous reddening, Galactic disk stars, random blends of red clump stars, correlated blends of red clump stars (binaries), evolution of the red clump stars, and red clump stars from a younger LMC stellar population. Combinations of these effects cannot be ruled out as the origin of this stellar population.

A natural interpretation of this new population is that it consists of red clump stars that are closer to us than those in the LMC. We derive a distance for this population of ~ 33 to 35 kpc, although the measurement is sensitive to the modeling of the LMC red clump component. We find corroborating evidence for this interpretation in Holtzman *et al.*'s (1997) *Hubble Space Telescope* CMD of the LMC field stars. The derived distance and projected angular surface density of these stars relative to the LMC stars ($\lesssim 5$ to 7%) are consistent with (1) models that attribute the observed microlensing lensing optical depth (Alcock *et al.* 1997) to a distinct foreground stellar population (Zhao 1997) and (2) tidal models of the interaction between the LMC and the Milky Way (Lin, Jones, & Klemola 1995). The first result suggests that the Galactic halo may contain few, if any, purely halo MACHO objects. The second result suggests that this new population may be evidence of a tidal tail from the interaction between the LMC and the Galaxy (although other interpretations, such as debris from the LMC-SMC interaction, are possible). We conclude that the standard assumption of a smoothly distributed halo population out to the LMC cannot be substantiated without at least a detailed understanding of several of the following: red clump stellar evolution, binary fractions, binary mass ratios, the spatial correlation of stars within the LMC, possible variations in the stellar populations of satellite galaxies, and differential reddening — all of which are highly complex.

1. Introduction

Identifying structure in the Galactic halo is critical to understanding the formation of the halo and to interpreting the microlensing observations that provide constraints on the composition of Galactic dark matter. Halo structures, such as tidal streamers, are the relics of the process of galaxy formation and, as envisioned in hierarchical models of the growth of structure, will testify to past and present accretion events. Furthermore, a concentration of stars in the halo will alter the microlensing optical depth along that line of sight and affect subsequent interpretations regarding the density of halo MACHO objects. These structures are difficult to identify because their stellar surface density is likely to be small. Therefore, large photometric surveys are required to identify these systems against the backdrop of halo stars (Johnston, Hernquist, & Bolte 1996). Our observations of the Large Magellanic Cloud (LMC) provide *UBVI* data for nearly 1 million stars (Zaritsky, Harris, & Thompson 1997) and an opportunity to search for intervening populations along the line of sight to the LMC.

As satellite galaxies or proto-galactic fragments interact with the Galaxy, tidal debris will be strewn through the halo. Identifying these remains, particularly if the interaction occurred many Gyr ago, is difficult, but some evidence for such events exists. Two particular examples of ongoing interactions between the Galaxy and its satellites are well established: the gaseous Magellanic Stream (Mathewson, Schwarz, & Murray 1977) and the tidal extension of the Sagittarius dwarf galaxy (Ibata, Gilmore, & Irwin 1995; Mateo *et al.* 1996). Somewhat more tentative is the inference that ancient interactions led to the set of satellite galaxies and globular clusters that share two preferred orbital planes around the Galaxy (Kunkel 1979; Lynden-Bell 1982; Majewski 1994). These orbital planes are presumably also populated by individual stars that were tidally stripped from the original parent satellite. Attempts to detect stars in the Magellanic Stream (*e.g.*, Brück & Hawkins 1983), have not yet yielded positive results, leading some (*e.g.*, Meurer, Bicknell, & Gingold 1985; Moore & Davis 1994) to propose models in which the stream material is removed from the Clouds by ram pressure rather than by tidal forces. As the known coherent structures are studied further, and other structures are discovered, we will be able develop a clearer picture of the physics that led to the formation of the outer Galactic halo and the evolution of the Galactic satellites.

A key development over the past few years in the effort to determine the nature of Galactic dark matter has been the systematic discovery of microlensing events toward the LMC (cf. Alcock *et al.* 1996). However, the interpretation of those results hinges on models of the stellar distribution along the the line of sight. Zhao (1997) has demonstrated that the microlensing optical depth may be dominated by tidal debris from the interaction of the LMC with the Galaxy, rather than by halo MACHOS, even if such tidal material has a stellar surface density of only a few percent of the LMC stellar surface density. Therefore, a detailed determination of the stellar distribution along the line of sight to the LMC is essential before reaching conclusions regarding the origin, density, and mass of the lensing population.

In this paper, we present observations that can be interpreted as evidence for a stellar population at a distance of ~ 35 kpc toward the LMC. In §2 we discuss the data, possible alternative interpretations of observations, and the line-of-sight stellar density distribution that we derive from these data. Although we cannot definitely exclude alternative interpretations, the intervening population hypothesis is entirely consistent with the data. Other interpretations (*e.g.*, that there are a large number of red clump binaries in the LMC or that there is a problem with current models of red clump stellar evolution) are also physically interesting. In §3 we discuss the potential effect of this population on conclusions drawn from the observed microlensing of LMC stars, the possible origins of such a stellar population, and the implications for dynamical models of the tidal interaction between the LMC and the Galaxy or between the SMC and LMC. In particular, the location and projected density of the proposed foreground stellar population

are consistent with a model in which they are responsible for the microlensing detection rate toward the LMC (as discussed hypothetically by Zhao 1997) and with a model of the tidal interaction between the Galaxy and the LMC (Lin, Jones, & Klemola 1995). Finally, we discuss some future observations that may discriminate between the various interpretations of the current data.

2. The Observations and Apparent Stellar Line-of-Sight Distribution

Our data come from digital, *UBVI*, drift scan images of a $2^\circ \times 1.5^\circ$ region located $\sim 2^\circ$ northwest of the center of the Large Magellanic Cloud. These data are part of an ongoing survey conducted at the Las Campanas 1-m Swope telescope that is designed to image the central 8° by 8° of the LMC and 4° by 4° of the SMC in the *UBVI* bandpasses using the GCC drift-scan camera (Zaritsky, Shtetman, & Bredthauer 1996). The effective exposure time is defined by the time required for the sky to drift across the field-of-view of the stationary telescope (~ 240 sec at the declination of the Clouds). The CCD has a 0.7 arcsec pixel $^{-1}$ scale, and the typical seeing at the telescope is between 1.2 and 1.8 arcsec. These data were obtained during Nov. 13-23, 1995. The details of the data reduction, the photometric and astrometric precision, and the photometric completeness are discussed by Zaritsky, Harris, & Thompson (1997).

We apply additional criteria to the existing catalog of stellar photometry. First, we only analyze stars for which magnitudes are available in all four filter bands and for which the *V* magnitude is brighter than the 50% completeness limit, $m_V = 21$ mag (see Zaritsky, Harris, & Thompson for details). Second, to minimize the number of stars that may have been mismatched between images taken in different filter bandpasses, we fit blackbody curves to all of the remaining stars. Because blackbody curves does not describe the full complexity of a stellar spectrum (*e.g.*, they lack absorption lines), fits with $\chi^2 > 1$ are generally acceptable. We interactively determine that stars with fits that have $\chi^2 \lesssim 30$ are acceptable and remove stars from the sample with best fits that have $\chi^2 > 30$. The fraction of “stars” removed from the sample due to this criterion is small (0.02).

To examine the distribution of stars along the line of sight, we use the most distinctive and common stellar population in the bright ($V > 21$) portion of the LMC color magnitude diagram (CMD) — the red clump stars — as a tracer of the full stellar population. We assume that red clump stars are standard candles. This assumption has been made by other investigators to examine the structure of the SMC (Hatzidimitriou and Hawkins 1989) and the Galactic bar (Stanek *et al.* 1997). These papers, and the references therein, argue that the luminosity of the red clump is relatively insensitive to age and metallicity if the stellar population is older than 1 Gyr (models predict luminosity changes $\lesssim 0.6$ mag for a given metallicity; Sweigart 1987).

Even if one accepts that red clump stars are fair standard candles, this approach to deriving the line of sight stellar density has some difficulties. For example, red clump stars and stars at the base of the red giant branch can be confused because the two populations have similar $B - V$ colors. To increase the distinction between these populations, we define a new color, constructed from a combination of the available four filter photometry, that maximally separates stars along the color axis in the red clump and the red giant branch portion of the CMD. We found the $U - V, B - I$ color-color plot to provide the greatest discrimination between the two evolutionary phases. Other choices, such as $U - B, V - I$, do not produce as significant a color variation as $U - V, B - I$ for these stars. To align the maximum dispersion of the stellar distribution along one axis, we apply a rotation to the color-color space. The axis with maximum dispersion defines our new color, $C \equiv 0.565(B - I) + 0.825(U - V + 1.15)$. We do not correct for extinction and justify this omission below.

The resulting Hess diagrams for the B , V , and I data near the red clump region are presented in Figure 1. The diagrams are created by modeling each star as a two-dimensional Gaussian with dispersions given by the photometric errors. All of the stars are summed to generate the density-coded CMD (or Hess diagram). In the V -band panel, we label the four features of interest: (1) the central red clump (RC), (2), the vertical extension of the red clump (VRC), (3) the red giant branch bump (RGBB; see King *et al.* 1985; Fusi Pecci *et al.* 1990), and (4) the giant branch (the unresolved combination of the red giant and asymptotic giant branches). Our claim, which we will attempt to justify to the reader, is that the VRC is real and that it consists of foreground red clump stars. We discuss the relative merits of various interpretations of the VRC next.

a) The VRC is spurious.

Is the VRC truly a distinct component or merely an artifact of the photometric uncertainties? We argue that the VRC is real due to its presence in the data from each of the four filter bands. To quantify this statement, we consider the magnitude distribution of stars in a vertical (*i.e.*, constant color) band of the CMD that includes the red clump stars. The boundaries of this region are taken as $2.85 < C < 3.57$, where C is the color defined above. This color range is selected to straddle the centroid of the RC distribution. The local minimum in the color distribution of stars with $18 < V < 18.6$ defines the boundary between the VRC and the RGBB and sets the red end of the color range. We define the blue end to produce a symmetric color range about the peak of the red clump distribution.

To demonstrate that the VRC feature exists in the data for the different filters, we plot in Figure 2 the distribution of the magnitude differences, Δm , between the stars in this color range and the magnitude of the RC peak. In all four bands, the Δm distribution is asymmetric, and, ignoring the U data for which the photometric uncertainties are significantly larger, the distribution has a shoulder at $\Delta m \sim -0.9$. For comparison, we superpose the I -band Δm distribution as a dotted line onto the B and V -band distributions. In contrast to the color-independence of the VRC, the position of the RGBB relative to the RC changes among the different filters (see Figure 1). Given that (1) the photometry from each of the four filters is independent, (2) the amplitude of the photometric errors is different in the four filters, (3) the extended feature in the magnitude distribution is asymmetric to *bright* magnitudes, (4) there is a minimum in the color distribution of stars with $18 < V < 18.6$ between the VRC and the RGBB, and (5) the VRC is fixed relative to the RC in the B -, V -, and I -band data while the RGBB moves, we conclude that the VRC is a real feature and distinct from the RGBB.

b) The VRC is due to clumpy extinction.

Could a clumpy intervening dust distribution, either in the Galaxy or the LMC, introduce sufficient scatter among the magnitudes of the RC stars to produce the VRC? The extinction required to produce the VRC (a ~ 0.9 mag offset in V) would produce $E(B - V) = 0.3$ and $E(B - I) \sim 1$ mag (for a standard extinction law; cf. Schild 1977). If such extinction were the cause of the VRC, then the magnitude offset, Δm , between the RC and the VRC would be 1 magnitude greater in B than in I . From the comparison of the magnitude distributions in Figure 2, it is evident that such large color differences are not present. We conclude that differential extinction is not responsible for the VRC.

c) The VRC is due to Galactic disk contamination.

Could the VRC be due to contamination from nearby Galactic stars? Such a component would need to have the colors of the LMC red clump stars, while being intrinsically significantly fainter, and to have some structure in the CMD in order to create a bump at the position of the VRC. Red dwarf stars at the main sequence turnoff may be a viable candidate. Main sequence K2V stars, which have the $B - V$ color of the RC, would have to lie at the unlikely distance of 2.3 kpc to match the magnitude of the VRC

stars ($V \sim 18.3$). Even if there is such a population of stars, would its distribution in the CMD have a fairly distinct break to create the shoulder observed in the Δm distribution (Figure 2)? The main sequence turnoff, if the turnoff is located at $B - V \sim 0.9$ and at a V magnitude that is 0.9 mag brighter than the LMC RC, might create the required break. The oldest main sequence turnoff stars in the Galactic disk population have an age of ~ 10 Gyr (as suggested by the oldest white dwarf stars; Wood 1992). Therefore, main sequence turnoff stars must be as red or bluer than 10 Gyr old main sequence stars, which have $B - V = 0.62$ (Straižys 1995). Because the RC has $B - V = 0.9$ and the VRC has the same color as the RC to within 0.07 mag (see below), main sequence turnoff stars cannot be responsible for the VRC. We conclude that Galactic foreground stars are not responsible for the VRC because (1) stars with the proper colors are not expected to have any distinguishing distribution in the CMD and (2) the stars with a possible distinguishing distribution have the wrong colors.

d) The VRC is due to stellar evolution.

Could the VRC be a feature created by the evolution of red clump stars, presumably upward from the RC to the VRC? As RC stars evolve, they move within a limited, but noticeable, region of the CMD (Seidel, Demarque, & Weinberg 1987; Sweigart 1987). Models for the evolution of RC stars demonstrate that their evolution proceeds primarily along the magnitude axis (*i.e.*, the color evolution can be relatively limited for particular choices of stellar parameters). Although these authors do not produce synthetic CMDs, the evolutionary tracks they present indicate that the luminosity increase necessary to populate the VRC (0.9 mag) is not caused by the stellar evolution of clump stars. The maximum change predicted by Sweigart for a metallicity, Z , of 0.01 (roughly appropriate for the LMC; Westerlund 1997) is about 0.6 mag, with a typical value being 0.3 mag. Synthetic $B - V$, V CMDs generated by Catelan & de Freitas Pacheco (1996) confirm this conclusion.

Could the VRC stars be composed of a younger LMC stars that have a more luminous red clump phase? To examine whether another LMC stellar population can create a second clump that is 0.9 mag brighter than the principal red clump, but that has the same colors, we examined Bertelli *et al.*'s (1994) isochrones. We chose an isochrone with $Z = 0.008$ and $\log(\text{age}) = 9.4$ as the best match to the giant branch morphology. Isochrones of younger stars ($\log(\text{age}) = 8.6$) have a red clump phase that is ~ 0.9 mag brighter, but the difference in $B - I$ colors between the two red clumps is about 0.2 mag. The observed $B - I$ color difference between the RC and VRC is $\lesssim 0.07$ mag (see below).

Based on the failure of the stellar evolution models to produce a population of stars that is brighter than the RC stars by 0.9 mag and that has the same $B - I$ color as the RC stars (within 0.07 mag), we conclude that neither stellar evolution within the clump nor the presence of a younger stellar population is responsible for the VRC. We caution that current stellar models, which include implementations of semiconvection, are complex and not necessarily definitive, and that we explored a limited set of models.

e) The VRC is due to stellar blends.

Could the blending of two stars into one apparent star create VRC “stars”? In the Magellanic Cloud, stellar fields are crowded and some blends undoubtedly occur. If the VRC “stars” are blends, then the unblended components presumably have quite different photometric properties. The simplest way for a blend to have the same colors as the RC is if the blended components are both RC stars. Such blends are reasonable because the RC is the dominant stellar component at these magnitudes (see Zaritsky, Harris, & Thompson 1997). Blends of RC stars with much fainter main sequence stars are irrelevant because they will not alter the apparent luminosity of RC stars sufficiently. Blends with other luminous stars (*e.g.*, young main sequence stars or red giants) will produce “stars” with a wide range of colors. Therefore, we consider only two types of RC-RC blends: (1) the random blend, in which stars are physically unassociated but

happen to lie sufficiently close to the same line of sight, and (2) the correlated blend, in which the two stars are physically associated.

We estimate the effect of random blended pairs of RC stars by adding artificial RC stars to our images. The magnitude of the artificial stars is set equal to the centroid of the RC distribution. We add 500 stars to a V -band subimage from our survey that has roughly 17,000 identified stars using DAOPHOT’s ADDSTAR procedure (Stetson 1987). We then process the photometry for the image as was originally done for the true data (Zaritsky, Harris, & Thompson 1997). The result from the 10 realizations of this test are shown in Figure 3, where we plot (1) the observed distribution (solid line), (2) the resulting distribution of measured magnitudes for the simulated stars (dotted line), and (3) the distribution of measured magnitudes if the simulated stars are distributed along the line of sight in a disk with a vertical (i.e. line-of-sight) scalelength of 5.3 kpc (dashed line), chosen to produce a close match to the peak of the observed distribution.

The dashed line distribution is an overestimate of the effect of blending for two reasons. First, we have adopted the photometric errors from the original simulations. For the model in which we distribute the RC stars along the line of sight, the relevant stars, in terms of the VRC, are those stars that are placed closer to us and are therefore brighter than the RC centroid (*i.e.*, at $\Delta m < 0$). These stars will be affected less by blending than in the original simulation because they are now brighter. Second, the density of simulated RC stars is more than four times larger than in the real data, so RC-RC blends are overrepresented. Even when overestimating the blending effect, we cannot reproduce the asymmetric distribution out to $\Delta m = -0.9$. We conclude that random blends are not responsible for the VRC.

If the RC stars are clustered, then blends will be more common than predicted in the random distribution model described above. Unbound pairs of stars with velocity dispersions $> 1 \text{ km sec}^{-1}$ will quickly ($\sim 2 \times 10^5 \text{ yrs}$) separate by more than 1 arcsec and become unblended in the images. Therefore, if tightly correlated RC blended pairs exist, they must be bound binary systems.

There are empirical and theoretical arguments against the presence of a significant number of RC binaries. We begin with an empirical argument. In the upper panels of Figure 4, we show the observed Δm distribution for stars in B , V and I . We subtract the RC contribution in two different ways. In the first case, we model the RC distribution using a Gaussian to represent the upper portion of the peak and an exponential to represent the tail of positive Δm values. We adjust the model parameters to provide the best fit both to the upper portion of the distribution and to the positive tail. The residuals from this model are shown in the middle panels. In the second case, we assume that the RC distribution is symmetric in magnitude about the peak and use the faint half of the distribution to define the RC contribution to the bright half of the distribution. We do not apply this method to the B data due to incompleteness at $\Delta m_B \sim 1$. The residuals from the symmetry model are shown in the bottom panels of Figure 4. Although neither method is ideal because of the assumption of a symmetric RC distribution, both methods will most likely underestimate the contribution of the RC at $\Delta m < 0$, because contamination from some blends and younger stars probably extends the bright tail of the RC distribution.

We measure the position of the peak of the residual distributions using a parabolic fit within $\pm 0.3 \text{ mag}$ of the peak. The peak positions, as measured in all three filters, are within $-0.91 \text{ mag} < \Delta m < -0.84 \text{ mag}$. These measurements place the residual peak systematically at brighter magnitudes than the expected position of RC-RC binary stars ($\Delta m = -0.75$ because the blended star is twice as luminous). The expected distribution of RC binaries is shown by the dashed lines (modeled to have the same shape as the central RC distribution and height equal to the residual distribution in the middle panels for comparison). These measurements also demonstrate that the relative colors of the RC and VRC do not differ by more than 0.07 mag from B to I .

There is a consistent offset between the position of the observed Δm distribution and that expected for a RC-RC binary population, but systematic problems remain. The residual stellar distribution is sensitive to the adopted shape of the RC star distribution, which is unknown. In addition, there is a general “background” distribution of stars throughout the CMD that is not modeled. This background is unlikely to be critical because any such background component will probably increase in density toward fainter magnitudes, and its removal would only push the observed residual peak to brighter magnitudes. Nevertheless, there are sufficient systematic uncertainties that the 0.1 mag offset is only suggestive evidence that these stars are not RC-RC binaries.

A theoretical argument against large numbers of RC binaries rests on the fine evolutionary timing required to get two stars in the RC phase at the same time. The timing requirement can be converted into a statement about the relative masses of the progenitor stars. The bulk of RC stars have progenitors with main sequence lifetimes in the 1 to 4 Gyr range (in order to match the increase in the star formation efficiency in the last few Gyr inferred by several previous investigators for the LMC, cf. Gallagher *et al.* 1996)). If two stars are going to reach the red clump phase at the same time, then their main sequence lifetimes must differ by less than the red clump phase lifetime. Therefore, the maximum allowed percentage difference in their main sequence ages, $\sim 5\%$, is given by the ratio of the red clump lifetime, 10^8 years (cf. Castellani, Chieffi, Pulone 1991), to the main sequence lifetime, t_{ms} . Using the relationship that $t_{ms} \propto (M/M_{\odot})^{-3}$ for stars somewhat more massive than the Sun (cf. Mihalas and Binney 1981), the upper limit on the mass difference of the two progenitor stars is 2%. Therefore, to account for the VRC with RC binaries implies that roughly 10% of all RC stars are in binary systems in which the progenitor masses differed by $\lesssim 2\%$. We reject this explanation due to the high degree of fine tuning necessary in the binary star mass ratios.

f) The VRC is due to foreground RC stars

Could the VRC stars be RC stars that are brighter than the LMC RC because they are nearer to us? To investigate this hypothesis, we have converted the magnitude differences for each star relative to the LMC RC centroid into a distance by assuming that all RC and VRC stars share the same absolute magnitude and that the centroid of RC stars lies at the distance of the LMC (50 kpc; Feast & Walker 1987). We have also corrected the observed number counts at each distance to a stellar density by accounting for the differential volume (our fixed area of sky contains different volumes at different distances). The inferred line-of-sight stellar distributions are shown in the top panels of Figure 5. The B , V and I distributions have a clear shoulder at a distance of about 35 kpc. Because the seeing is the worst in U , the photometry is also the worst, and the features are broader and weaker. Nevertheless, when we fit the simple model described below, we find that the excess stellar density due to the VRC is present in all four filters. The centroid of the VRC, as determined from a parabola fitted to the stellar density distribution between 30 and 40 kpc (and between 25 and 45 kpc for the U band data due to the less pronounced peak), is at 33.7, 35.0, 34.8, 34.1 kpc for $UBVI$, respectively. The peak is at 33 kpc if one adopts $\Delta m = -0.9$ as the centroid of the population and *does not* correct the density for volume effects. The latter approach is appropriate if the magnitude distribution around the VRC peak does not arise from differential distances relative to the VRC centroid.

The model shown in Figure 5 (solid line), is a combination of three components: (1) a Gaussian, with a dispersion chosen to fit the peak of the distribution, (2) an exponential, with a scalelength chosen to generate the extended tail beyond 50 kpc, and (3) a power-law foreground component, with an index chosen to account for the sharp rise of objects at small distances. The exponential is fit to the faint tail of the stellar distribution between 50 and 60 kpc. We ignore the data corresponding to inferred distances greater than 60 kpc, because the magnitude cuts originally applied to define the sample exclude such distant RC

stars. The model exponential has the same scale-length (4.5 kpc) for all four filters. This value should, for the purposes here, be considered only as an empirical quantity that is a good fit to the data, rather than necessarily having physical significance. We adopt an exponent of -0.95 for the power-law component in all four filters, again as an empirical fit. The color of the stars responsible for the power-law component depends slightly on magnitude, so the number represented at any distance in Figure 5 is not a constant fraction of the total population. Therefore, the exponent should not be interpreted physically.

The agreement among distances measured in each of the four filters, and among the amplitudes of the residual distributions in B, V, and I, is consistent with the interpretation of the VRC as an intervening population in the line of sight to the LMC. We estimate the projected angular stellar density of such a foreground population relative to that of the LMC by comparing the number of stars in the VRC with the number of stars in the RC. This estimate is highly model dependent because both the RC and any foreground component must be subtracted from the observed distribution of stars. Nevertheless, we use the models just described and estimate that the VRC has a projected angular number density of ~ 5 to 7% of the LMC RC stars. This value is most likely an overestimate for at least two reasons: (1) due to stellar evolution, blends, and binaries (which all work to generate stars that are brighter than the RC centroid), the RC is probably more extended toward $\Delta m < 0$ than the symmetric model implies and (2) the RGBB is likely to partially pollute the region of the VRC.

2.1. A Corroborating Observation: The Lower Main Sequence

If the VRC is a manifestation of a population between us and the LMC, then the entire LMC CMD diagram should contain traces of a parallel CMD, shifted in magnitude by about 0.9 mag. We have searched for evidence of a parallel RGB, but are unable to draw any conclusions due to the steepness of the RGB and our photometric uncertainties, which would obscure a faint foreground population. The upper main sequence is also not useful for this exercise, because it is nearly vertical in our CMDs. Our only remaining option is to examine the lower main sequence, but the sensitivity limit and photometric errors of our data preclude their use for such a study. Instead, we examine HST data of the field population in the LMC generously provided by J. Holtzman (the data are discussed and analyzed by Holtzman *et al.* 1997).

The $V - I, I$ CMD from Holtzman *et al.* is shown in Figure 6. There is a faint trace of a secondary main sequence (it is visible over the range $0.6 < V - I < 1$ where the main sequence stars are well below the turnoff magnitude and the photometric errors are still small). Differential reddening is not responsible for the apparent gap between the main sequence and the secondary sequence, because the reddening vector is nearly parallel to the main sequence. Models presented by Holtzman *et al.* (their Figure 4) to study the star formation history of the LMC illustrate that neither metallicity nor age variations between populations will populate the apparent secondary sequence.

There are two quantitative consistency checks on the hypothesis that the secondary sequence is drawn from the same foreground population as the VRC. First, the secondary sequence should appear ~ 0.9 mag above the main sequence. Second, the secondary population should have a projected angular number density of $\lesssim 5$ to 7% of that of the principal population. For these tests, we define a fiducial main sequence by measuring the mode of the stellar colors in magnitude bins for the main sequence stars and by then fitting a second order polynomial as a function of color to the magnitudes. Our resulting fiducial main sequence is $M_V = -3.26 + 19.66(V - I) - 9.99(V - I)^2$. For each star between $0.7 < V - I < 0.9$ and $3.5 < M_V < 7.25$, we evaluate the magnitude difference relative to the fiducial main sequence. We set the blue color limit to avoid confusion with the subgiant branch at bright magnitudes and set the red color limit to avoid being seriously affected by photometric errors. The distribution of magnitude differences,

for both the observations and simulated data are in Figure 7 (see Holtzman *et al.* for details regarding the simulation).

The observed data clearly contain a secondary peak at $\Delta m \sim -0.8$. The position of the residual peak as predicted by the VRC is shown by the arrow, with the differences in positions among the four filters illustrated by the horizontal error bar. Any attempt to subtract the contribution from the principal main sequence will shift the secondary peak toward $\Delta m = -0.9$, in even better agreement with the position of the VRC (note that in Figure 2, before any RC “background” subtraction is attempted, the VRC is also closer to $\Delta m = -0.8$). No such peak is observed in the simulations (the peak at $\Delta m = -0.6$ mag is not significant at the 2σ level, while the observed peak is significant at $> 4\sigma$). As for the VRC, determining the number of stars in this secondary peak requires modeling of the primary peak. After crudely modeling the contribution of the principal main sequence as half of the signal seen in the secondary peak, we estimate that the angular stellar density of the secondary population is $\sim 4\%$ of the LMC’s (if the contribution from the LMC main sequence to the secondary peak is negligible, then the percentage increases to $\sim 8\%$). *Therefore, both the position and amplitude of the secondary peak seen in the main sequence population are consistent with the values that one would predict from the properties of the VRC.*

The observation of a brighter population of stars in another part of the CMD greatly strengthens the case for an intervening population. and provides additional evidence against alternative interpretations for the VRC. First, neither stellar evolution nor metallicity effects can account for this parallel main sequence population (see Figure 4 of Holtzman *et al.* 1997). The presence of a younger population (which might affect the VRC) would have no effect on this portion of the main sequence. Second, blends are highly unlikely to be responsible for the parallel main sequence. Unlike in the VRC region of the CMD, where the red clump stars dominate and red clump-red clump blending will be the most common type of blend, there is no reason to expect main sequence stars to blend with stars of exactly the same magnitude (as required to create a distinct peak at $\Delta m \sim 0.8$ mag). Because the main sequence data come from HST observations and the VRC data come from ground based observations, it would be particularly unfortuitous for both data sets to have a similar blending problem for such different stellar populations. Finally, the possibility of binary stars, which is a much more likely explanation for the lower main sequence excess population (because the timing constraints are not rigid), is not a promising explanation of the VRC. For example, Rubenstein and Bailyn (1997) have observed the effects of binary stars on the CMD of a core-collapse globular cluster, NGC 6752. The signature they observe, an asymmetric expansion of the main sequence toward redder and brighter objects, is similar to that described here. However, if one invokes this explanation for the lower main sequence excess population, another explanation is necessary for the VRC. Such hybrid explanations for the two populations are certainly possible, but become increasingly unappealing as more complications are added.

3. Implications

3.1. For MACHO Microlensing Experiments

The MACHO collaboration has measured an optical depth to microlensing of $2.9_{-0.9}^{+1.4} \times 10^{-7}$ for events between 2 and 200 days toward the LMC (Alcock *et al.* 1997). The subsequent interpretation of that result relies on models of the stellar and dark matter halo distributions. Any irregularity in the density of lenses in the halo, especially one that would be expected to correlate with the position of the Large Magellanic Cloud, would seriously affect any interpretation. Zhao (1997) demonstrated that a stellar stream from a proto-LMC that was originally twice as massive as the current LMC could provide the necessary

microlensing optical depth. Such models imply that MACHOS comprise at most a small fraction of the Galactic halo.

We can straightforwardly estimate the optical depth to microlensing, τ_μ , of the putative intervening population toward the LMC using

$$\tau_\mu = 4\pi G \Sigma D_{LMC} x(1-x),$$

where Σ is the surface mass density of the lenses, D_{LMC} is the distance to the LMC, which is taken to be 50 kpc (Feast & Walker 1987), and x is the ratio of the distances between the sources and the lenses. For a population at 35 kpc, this equation can be rewritten as

$$\tau_\mu = 7.5 \times 10^{-9} \Sigma,$$

where Σ is in units of M_\odot/pc^2 . To estimate the surface mass density of the foreground population, we assume that its stellar population is identical to that of the LMC. Our observed field spans a range in radius of ~ 1 to 3 kpc (in the LMC disk plane these radii correspond to 1.8 and 5.5 kpc for our adopted LMC inclination of 33°). We estimate the average surface mass density of the LMC using the rotation curve and assuming that dark matter makes a negligible contribution to the rotation curve at these radii. Luks and Rohlfs (1992) present a rotation curve for the disk of the LMC that has a roughly flat rotation curve with a velocity of 70 km sec^{-1} at these radii. Adopting the simple spherical formula, $M = rv^2/G$, implies a mass in this annulus of $4.0 \times 10^9 M_\odot$. Projecting this mass on the observed annulus from 1 to 3 kpc results in an average projected surface mass density of $159 M_\odot/\text{pc}^2$. If the foreground population is 5% of the projected angular surface number density of the LMC population (see §2), then the surface mass density of the foreground component would be $8 M_\odot/\text{pc}^2$ if it was at the distance of the LMC. However, 1 pc^2 at 35 kpc corresponds to 2 pc^2 at 50 kpc, so the mass surface density of the inferred foreground population is $16 M_\odot/\text{pc}^2$. This surface mass density translates to $\tau_\mu = 1.2 \times 10^{-7}$, or about half of the measured value (but only 2σ away using only the uncertainty in the MACHO microlensing optical depth).

We conclude that inferences regarding the halo MACHO population depend critically on the characteristics of the putative foreground population. Limits that constrain the foreground population to well under 5% of the LMC angular stellar density (in the region of the LMC that we observed) are required to reach the conclusion that the microlensing observations necessarily imply the presence of purely halo MACHOS. *Even if an alternate interpretation for the observations discussed in this paper proves to be principally correct, we conclude that placing limits on foreground populations within 20 kpc of the LMC is extremely complicated and requires a detailed understanding of stellar evolution, binary fractions, binary mass ratios, stellar correlation functions, differences in the stellar populations among satellite galaxies, and reddening.*

3.2. For Dynamical Models of the Satellite Population

The origin of the proposed foreground stellar population is an interesting puzzle. There are at least three possibilities: (1) these stars are debris from the interaction between the LMC and the Galaxy, (2) these stars are debris from the interaction between the SMC and LMC, or (3) these stars belong to an unknown dwarf spheroidal galaxy, which currently may or may not be internally gravitationally bound. We briefly discuss possibilities (1) and (3), for which we have some additional constraints.

Is the observed population of intervening stars consistent with predictions of the position and density of the tidal tails produced in models of the interaction between the LMC and the Galaxy? First, we consider the position of the tidal streamer. Typical estimated positions resulting from the tidal model for the origin

of the gaseous Magellanic Stream place the inner stellar stream anywhere from 30 to 45 kpc (Lin, Jones, & Klemola 1995) — in agreement with our interpretation of the observations (a density peak at ~ 35 kpc). Second, we consider the density of stars along the hypothesized stream. In §2 we measured that the VRC has a projected angular surface density of 5 to 7% that of the LMC. The HST data from observations of the lower main sequence support this value. The HST measurement of the foreground stellar density is important because it is obtained from main sequence stars rather than RC stars, and so, it is less affected by possible population differences between the foreground population and the LMC stars. Unfortunately, the surface density is only a weak constraint on the models because the parameters of the progenitor satellite galaxy are unknown.

Assuming that the foreground population is a tidal streamer, we can estimate the mass of the original satellite galaxy from the current surface density of the proposed foreground component. The stars escaping from a tidally stripped galaxy follow an orbit similar to that of the parent galaxy (cf. Johnston, Hernquist, & Spergel 1995). If stripped stars from the LMC have velocities that differ by 100 km sec^{-1} , these stars would wrap around the Galaxy at a radius ~ 35 kpc within 2.5 Gyr. Along segments of these streams of stellar debris, the local velocity dispersion perpendicular to the “orbit” is comparable to the virial velocity of the parent galaxy prior to the tidal disruption (Oh, Lin, & Aarseth 1995). Consequently, the width of the stream, normal to its orbital plane, is comparable to the size of the parent galaxy. During the final stage of tidal disruption, the total mass contained within the stream is comparable to that of the residual stars in the parent galaxy. In this limit, the ratio of projected stellar surface density along the stream to that in the parent galaxy is equivalent to the ratio of the angular extent of the parent galaxy to 2π . The disk of the current LMC extends over ~ 14 degrees (Westerlund 1997), so a ring of material that has a total mass equal to the current LMC would have an angular projected surface density of $14/360$, or 4%. Therefore, the observed projected density of the foreground population is comparable to that expected if the population is the tidal debris of an LMC-like satellite, or a proto-LMC with twice the current LMC mass.

One possible problem for a tidal stream model is the lack of observed stars associated with the neutral hydrogen Magellanic Stream ((Brück & Hawkins 1983). Some authors (Meurer, Bicknell, & Gingold 1985; Moore & Davis 1994) have proposed models in which the gas is removed from the LMC by ram pressure stripping, in which case stars are not expected to be in the Stream. However, previous searches have focused on bright, early-type stars which will not be present if the gas was pulled out over 1 Gyr ago and there was no subsequent star formation. A few carbon stars with appropriate magnitudes have been found in the Stream (Demers, Irwin, & Kunkel 1993). However, the number of carbon stars detected is too small to make accurate estimates of the Stream’s stellar content. Because the intrinsic nature (and hence luminosity) of these stars is ambiguous, their distance cannot be reliably determined. Even if low mass stars are not found in the Stream, one might be able to account for the displacement of stars and gas by appealing to a low density gaseous Galactic halo that generates a mild drag on the neutral hydrogen.

Now we consider the possibility that the proposed foreground population is associated with a dwarf galaxy along the line of sight. We assume that the foreground stars, including the VRC, have a similar stellar luminosity function and mass-to-light ratio as those in the LMC. Therefore, the stellar surface mass density of the foreground population is $\sim 16 M_{\odot}/pc^2$ (see above). The surface number density of the VRC is not observed to vary over our field (2° , or 1.2 kpc at 35 kpc). If a similar spatial extent is assumed along the line of sight, the inferred mass density is $0.01 M_{\odot}/pc^3$. This density is a factor of five smaller than the *minimum* value of the central dark matter density found for the Draco and Ursa Minor dwarf spheroidals (models with isotropic velocity distributions predict mass densities of $\sim 1 M_{\odot}/pc$; Pryor & Kormendy 1990). Therefore, if the mass-to-light ratio in the foreground population is similar to that in Draco and Ursa Minor (~ 70 ; Olszewski, Aaronson, & Hill 1995), then this population has a mass density

comparable to the centers of dwarf spheroidal galaxies. At their present Galactic distance (~ 69 and 86 kpc, respectively; Cudworth *et al.* 1986; Nemec *et al.* 1988; Nemec 1985), Draco and Ursa Minor would be tidally disrupted by the Galaxy if they had no dark matter (Faber & Lin 1983, Oh, Lin, & Aarseth 1993). Therefore, the foreground population, which is at half the Galactocentric distance, would also be tidally disrupted unless it has substantial dark matter. If the hypothesized foreground population is traced over a larger radial range, then the inferred mass density would decrease (since the object would be thicker as well as wider) and even more dark matter would be required to keep it gravitationally bound.

4. Resolving the Question

There are several potential ways to discriminate between the various hypotheses for the origin of the VRC and the possibly related main sequence population. Because certain explanations (*e.g.*, blends, binaries, younger stellar populations) predict direct correlations between either the number of RC stars or OB stars and the number of VRC stars, observations of fields farther from the center of the LMC could verify or refute these hypotheses. We have attempted this test within our survey area by counting both RC and VRC stars on a 10 by 7 rectangular grid, statistically subtracting the RC component, and examining the scatter plot between RC and VRC number densities. Although we observe a slight anticorrelation between the two, supporting the hypothesis that the RC and VRC are unassociated and that the VRC is in the LMC foreground, the uncertainties in the statistical correction are sufficiently large to mask a correlation if present. If the VRC stars do not correlate with the number of RC stars, then a comparison of the number of VRC stars in outer LMC fields along the LMC orbit, to the number in fields perpendicular to the orbit, would establish whether the VRC is spatially distributed in a tidal stellar stream.

Other tests involve looking for variable stars in the microlensing databases. For example, the MACHO collaboration excludes the possibility of a dwarf galaxy along the line of sight between us and 30 kpc based on the analysis of ~ 6000 RR Lyrae stars (Minniti priv. comm). These investigators avoid the region within 20 kpc from the LMC due to the ambiguities in disentangling reddening, intrinsic scatter, and distance effects. Even without these problems, it is difficult to predict the magnitude of the expected signal in the RR Lyraes from the foreground population suggested by the VRC. There are several unknown factors that come into play. First, the ratio of the foreground to LMC populations can vary due to clumpiness in the foreground component or to variations in the LMC surface density. For example, the microlensing surveys have been more concentrated toward the LMC bar than our observations, so the foreground population in these data would be a smaller fraction of the total number of stars. Second, old stellar populations, such as RR Lyrae, generally have fairly steep radial density gradients ($\rho \propto r^{-3}$ for Galactic RR Lyrae (Oort & Plaut 1975) and $r^{-3.5}$ for globular clusters (Harris 1976)) so that tidally stripped material may have a lower RR Lyrae/main sequence ratio than the central LMC fields. Third, if the foreground population is not related to the LMC, then its RR Lyrae fraction is an unknown quantity and may be lower, or higher, than that in the LMC.

Radial velocity observations might be more successful at discriminating between models for the VRC. The radial velocity distribution of the proposed foreground stars might be expected to be significantly different than those of LMC RC stars. If VRC stars are members of a dwarf galaxy between the LMC and the Galaxy, their mean velocity may differ from that of the LMC RCs by up to 200 km s^{-1} with a relatively small dispersion. If the VRC stars are tidal debris from the LMC, they would have a relatively small mean velocity with a dispersion of up to 200 km s^{-1} . If the magnitude of VRC stars is a precise distance indicator, it may correlate with the radial velocity of the VRC star. Differences between the velocity distribution of the VRC and RC stars would support the idea that the VRC stars are not in the

LMC. A velocity distribution consistent with that of the LMC would be inconclusive.

5. Summary

We identify a previously unknown extension of red clump (RC) stars toward brighter magnitudes that lies ~ 0.9 mag above the red clump centroid in the CMD of the Large Magellanic Cloud. The extension appears in the photometry of all four filters, thereby confirming it as a real feature in the CMD. The color of the extension is the same as the RC to within ~ 0.07 mag over B , V , and I .

We explore various explanations of this feature, including unresolved stellar blends (both random and correlated), stellar evolution, composite stellar populations, patchy extinction, a Galactic disk population, and an intervening stellar population at a distance of about 35 kpc. The latter explanation is the most consistent with the data.

We found corroborating evidence for a foreground population in the HST CMD of field stars in the LMC provided by Holtzman (Holtzman *et al.* 1997). These data show a distinct sequence of stars that is parallel to, but brighter than, the bulk of the main sequence stars by ~ 0.8 mag. The magnitude offset and the relative projected density with respect to the principal LMC population are in agreement with the values measured from the vertically extended red clump (VRC) stars. Although there are explanations other than a foreground population for the VRC and the parallel lower main sequence, a single alternative explanation cannot reproduce both observations. Therefore, the similarity in the properties of the VRC and parallel main sequence suggests the existence of a foreground population at ~ 35 kpc.

If the intervening population exists, then what are the implications for (1) the interpretation of the microlensing rates toward the LMC and (2) the origin of this population? We estimate the microlensing optical depth of this population to be $\sim 1.2 \times 10^{-7}$. This optical depth is about one-half of the observed value (Alcock *et al.* 1996), but only 2σ from the observed value. Given the large uncertainties in the measured optical depth and in our measurements of the foreground surface mass density, it is plausible that the entire microlensing rate can be accounted for by normal stellar populations and that there is no need to invoke purely halo MACHOs.

We speculate that this population originates from the LMC-Galaxy interaction, the LMC-SMC interaction, or from an intervening dwarf galaxy (that is possibly tidally disrupted). Numerical simulations of the LMC-Galaxy interaction (Lin, Jones, & Klemola 1995) predict that a tidal tail might lie between 30 and 45 kpc (consistent with the distance of 35 kpc inferred from the peak of the VRC). The surface density constraints from such models are weak, because they depend on the unknown mass of the progenitor. However, if the original LMC had about twice its current stellar mass, the projected surface density predicted by a simple calculation is in agreement with the observations.

The existence of the VRC, and of its sister population near the lower main sequence, is clear, but the interpretation of these components is still ambiguous. The simplest explanation is that a stellar population lies in front of the LMC. This population may be the signature of a tidal tail from the LMC and may be responsible for the LMC microlensing events. In any case, we conclude that it is exceedingly difficult from the CMD alone to rule out a foreground population of stars at the few percent level. As a result, the issue of possible intervening populations along the line-of-sight and within ~ 20 kpc of the Large Magellanic Cloud is entirely open. Therefore, the observed microlensing rate toward the LMC should not yet be interpreted as evidence for a purely halo MACHO population, and second order results, such as the mass distribution of halo MACHOS, should be viewed with extreme caution. Fortunately, several tests of this hypothesis are feasible and should allow some progress on this issue within the next few years.

Acknowledgments: DZ gratefully acknowledges financial support from a NASA LTSA grant (NAG-5-3501) and an NSF grant (AST-9619576), support for the construction of the GCC from the Dudley Observatory through a Fullam award and a seed grant from the Univ. of California for support during the inception of MC survey. DZ also thanks the Carnegie Institution for providing telescope access, shop time, and other support for the MC survey. Finally, we thank A. Gould, P. Guhathakurta, and D. Minniti for helpful discussions and A. Zabludoff for a careful reading of a preliminary draft.

References

- Alcock, C. *et al.* 1997 preprint (astro-ph/9606165)
- Bertelli, G., Bressan, A., Chiosi, C., Fagotto, F., & Nasi, E. 1994, *AA Sup.*, 106, 275
- Brück, M.T. & Hawkins, M.R.S. 1983, *AA*, 124, 216
- Castellani, V., Chieffi, A., & Pulone, L. 1991, *ApJS* 76, 911
- Catelan, M., & De Freitas Pacheco, J.A. 1996, *PASP*, 108, 166
- Cudworth, K.M, Olszewski, E.W. & Schommer, R.A. 1986, *AJ*, 92, 766
- Demers, S., Irwin, M.J., & Kunkel, W.E. 1993, *MNRAS*, 260, 103
- Faber, S.M. & Lin, D.N.C. 1983, *ApJL*, 266, 17
- Feast, M., & Walker, A.R. 1987, *ARA & A*, 25, 345
- Fusi Pecci, F., Ferraro, F.R., Crocker, D.A., Rood, R.T., & Buonanno, R. 1990, *AA*, 238, 95
- Gallagher, J.S., *et al.* 1996, *ApJ*, 466, 732
- Hatzidimitriou, D. & Hawkins, M.R.S. 1989, *MNRAS*, 241, 667
- Harris, W.E. 1976, *AJ*, 81, 1095
- Holtzman, J. *et al.* 1997, *AJ*, 113, 656
- Ibata, R.A., Gilmore, G., & Irwin, M.J., *MNRAS*, 277, 781
- Johnston, K.V., Hernquist, L., & Bolte, M. 1996, *ApJ*, 465, 278
- King, C.R., Da Costa, G.S., & Demarque, P. 1985, *ApJ*, 299, 674
- Kunkel, W.E. 1979, *ApJ*, 228, 718
- Lin, D.N.C., Jones, B.F., & Klemola, A.R. 1995, *ApJ*, 439, 652
- Luks, Th., & Rohlf, K. 1992, *AA*, 263, 42
- Lynden-Bell, D. 1982, *Observatory*, 102, 202
- Majewski, S. 1994, *ApJL*, 431, 17
- Mateo, M. *et al.* 1996, *ApJL*, 458, 13
- Mathewson, D.S., Schwarz, M.P., Murray, J.D., 1977, *ApJL*, 217, L5
- Meurer, G.R., Bicknell, G.V., & Gingold, R.A. 1985, *PASAu*, 6, 2
- Mihalas, D., & Binney, J. 1981, *Galactic Astronomy*, (W.H. Freeman & Co.: San Francisco)
- Moore, B., & Davis, M. 1994, *MNRAS*, 270, 209
- Nemec, J.M. 1985, *AJ*, 90, 204
- Nemec, J.M., Wehlau, A., & del Olivares, C.M. 1988, *AJ*, 96, 528
- Oh, K.S., Lin, D.N.C., & Aarseth, S.J. 1995, *ApJ*, 442, 1420
- Olszewski, E.O., Aaronson, M., & Hill, J.M. 1995, *AJ*, 110, 5
- Oort, J.H., & Plaut, L. 1975, *AA*, 41, 71
- Pryor, C., & Kormendy, J. 1990, *AJ*, 100, 127
- Rubenstein, E.P. & Bailyn, C. D. 1997, *ApJ*, 474, 701

- Sahu, K. 1994, *PASP*, 106, 942
- Schild, R.E. 1977, *AJ*, 82, 337
- Seidel, E., Demarque, P., & Weinberg, D. 1987, *ApJS* 63, 917
- Stanek, K.Z. *et al.* 1997, *ApJ*, 477, 163
- Stetson, P.B. 1987, *PASP*, 99, 191
- Straižys, V. 1995, *Multicolor Stellar Photometry*, (Pachart Publishing House: Tucson)
- Sutherland, W., et al. 1997, in “Identification of Dark Matter”, in press.
- Sweigart, A. 1987, *ApJS* 65, 95
- Westerlund, B.E. 1997, *The Magellanic Clouds*, (Cambridge Univ. Press: Cambridge)
- Wood, M.A. 1992, *ApJ*, 386, 539
- Zaritsky, D., Shectman, S.A., & Bredthauer, G. 1994, *PASP*, 108, 104
- Zaritsky, D., Harris, J., & Thompson, I. 1997, in press
- Zhao, H. 1997 preprint (astro-ph/9703097)

Figure Captions

Fig. 1.—

Hess diagrams of the region including the red clump and giant branches in B , V , and I vs our modified color measure (*cf.* §2). The images are generated by creating a two-dimensional Gaussian with width and height defined by the observational uncertainties for each star, and then summing all of those Gaussians. In the upper panel (for the B -band data), we have placed vertical bars to indicate the color selection used to isolate the VRC and RC stars from the other populations. In the middle panel (for the V -band), we have labeled the various components discussed in the text. The vertical axis in each panel spans 3.5 mag. The diagram contains about 70000 stars.

Fig. 2.—

The distribution of magnitudes relative to the magnitude of the RC centroid. For each of the four filters we show the distribution of stellar magnitudes within the color bin $2.85 < C < 3.57$. In the B and V panels, we have overplotted the I -band distribution for comparison as the dotted line. The B , V , and I panels also have a vertical line showing the position of the VRC centroid ($\Delta m \sim -0.9$).

Fig. 3.—

The effect of random blends. We summarize the results of our artificial star tests. The solid smooth curve the V -band distribution is from Figure 2. The dotted line shows the result of adding 5000 stars with the magnitude of the red clump centroid to the survey images and remeasuring the magnitudes (*i.e.*, for no errors, the distribution would be a delta function at $\Delta m = 0$). The dashed-line histogram shows the results of expanding the simulated distribution by modeling the RC stars as having an exponential distribution along the line-of-sight with a scaleheight of 5.3 kpc (selected to provide a good empirical match to the observed distribution). For two reasons, this test is expected to be an overestimate of the effect of blends (see text).

Fig. 4.—

The Δm distribution for the B , V , and I photometry. In the upper panels, we present the data (solid line) and the Gaussian+exponential models as described in the text (dashed line). In the middle panels, we present the residuals (solid line) from the models drawn in the upper panels. Also in the middle panels, we present for comparison the expected distribution of RC-RC blends, normalized to the height of the observed residuals and to the width of the principal RC peak. In the lower panels, we present the residuals (solid line) for a second RC model, the symmetry model (see text). Again, the expected distribution of RC-RC blends is plotted for comparison (dashed line).

Fig. 5.—

The line of sight density distribution of stars. The magnitude distribution of stars within the color bin described in §2 is converted to a distance distribution assuming that all stars have the same absolute magnitude and that it is equal to that of the centroid of the RC distribution. The density at each radius is corrected for the volume surveyed at that distance. The upper panels show the distribution for photometry in each filter (dotted lines) and the model (see text; solid line). In the lower panel, we show the residual

after subtracting the model. The dotted line is the U data, short-dash/long-dash line is the B data, short-dash line is the V data, and long-dash line is the I data.

Fig. 6.—

The V, I color-magnitude diagram of the LMC field population from the data of Holtzman *et al.* (1997). The secondary sequence is most clearly visible at about $V - I = 0.8$ and $V = 5.3$.

Fig. 7.—

The line of sight density distribution of main sequence stars from Figure 6, and the Holtzman *et al.* (1997) simulation of this population calculated as described in the text. The arrow indicates the position of the foreground population as expected from the VRC centroid. The horizontal errorbar attached to the arrow indicates the spread in positions derived for the VRC from the data in different filters.

Fig. 1.—

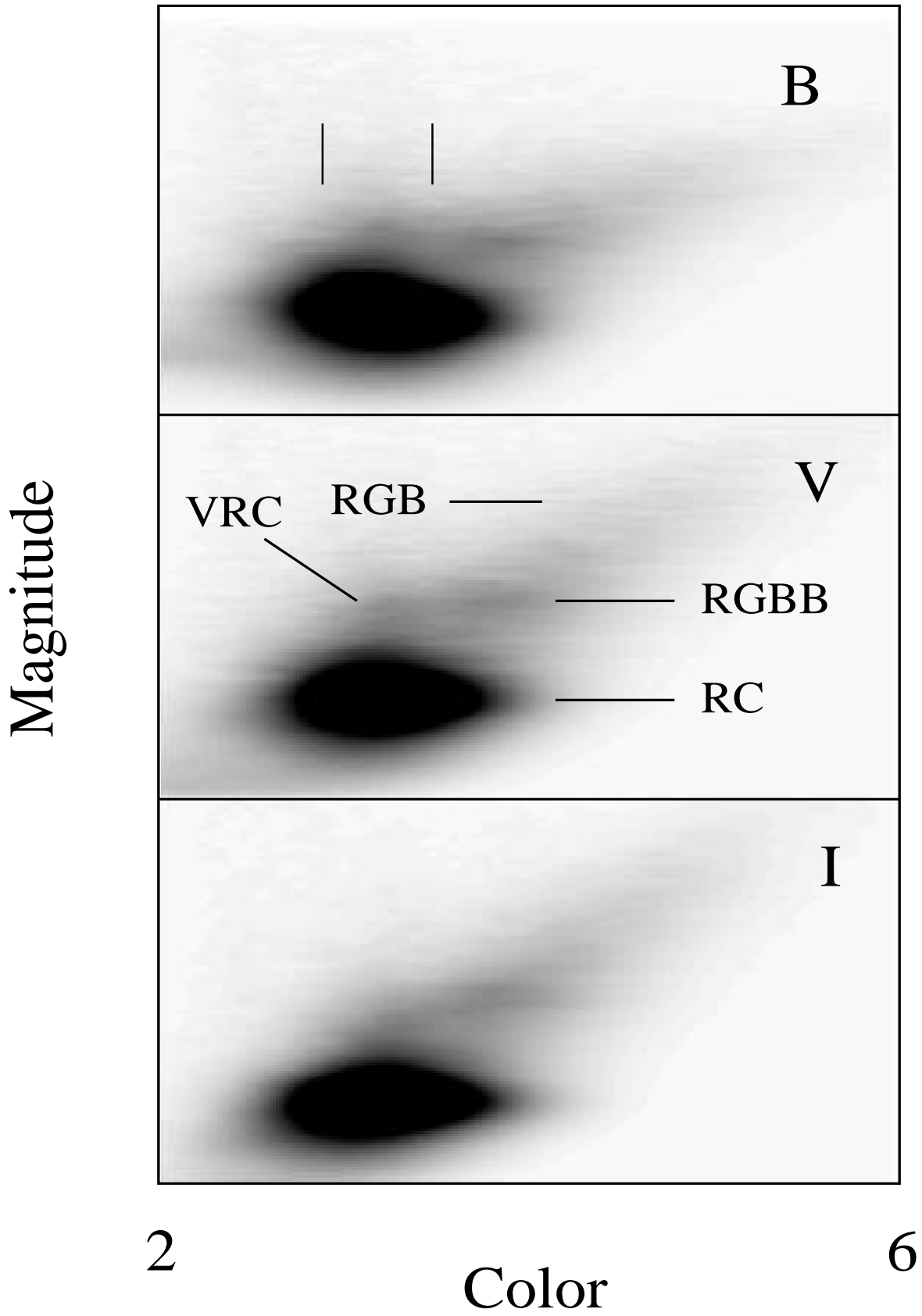


Fig. 2.—

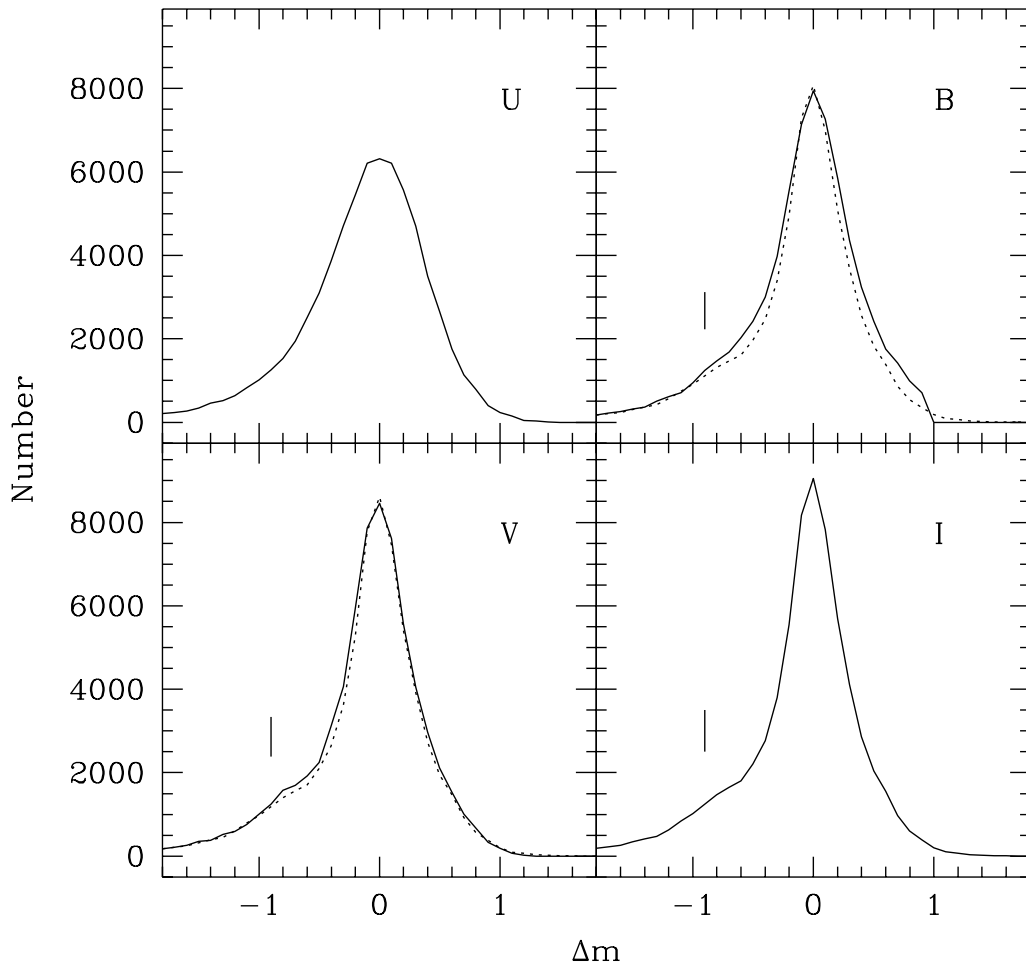


Fig. 3.—

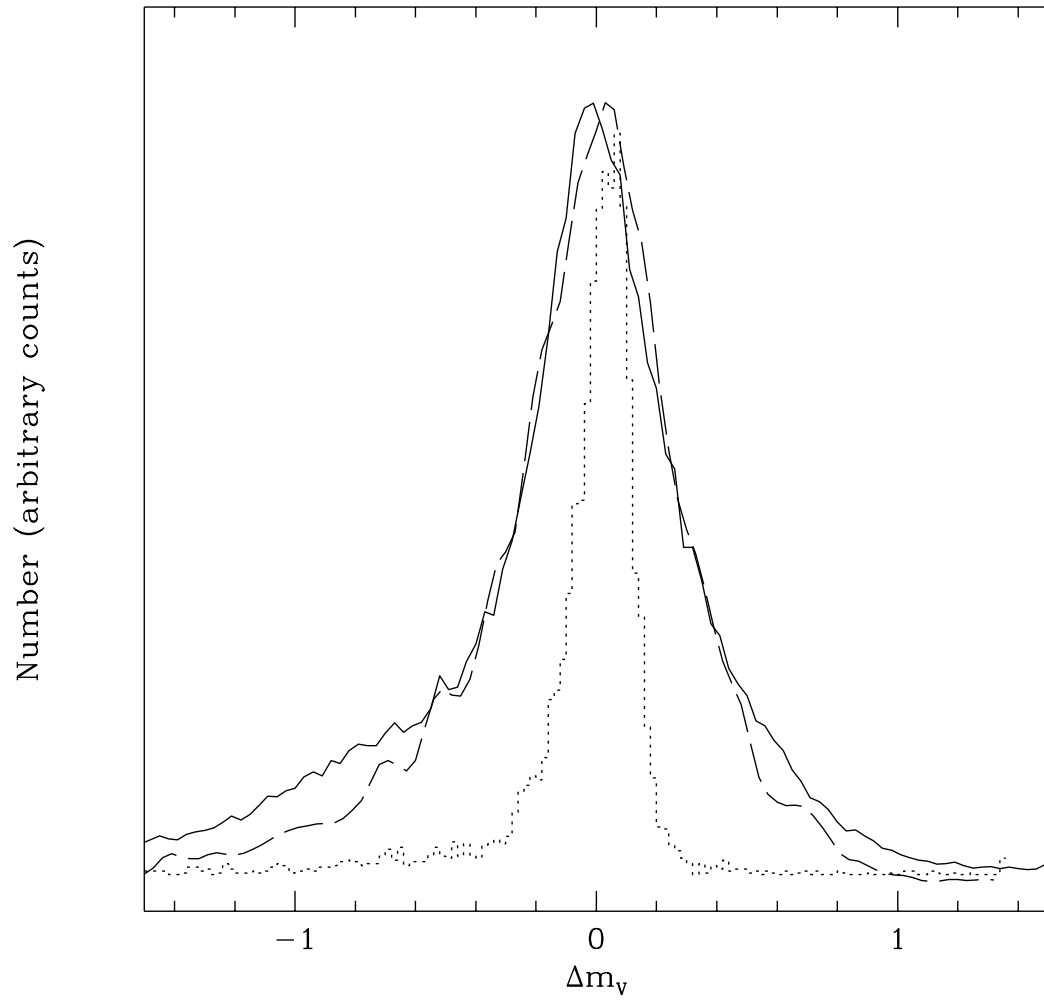


Fig. 4.—

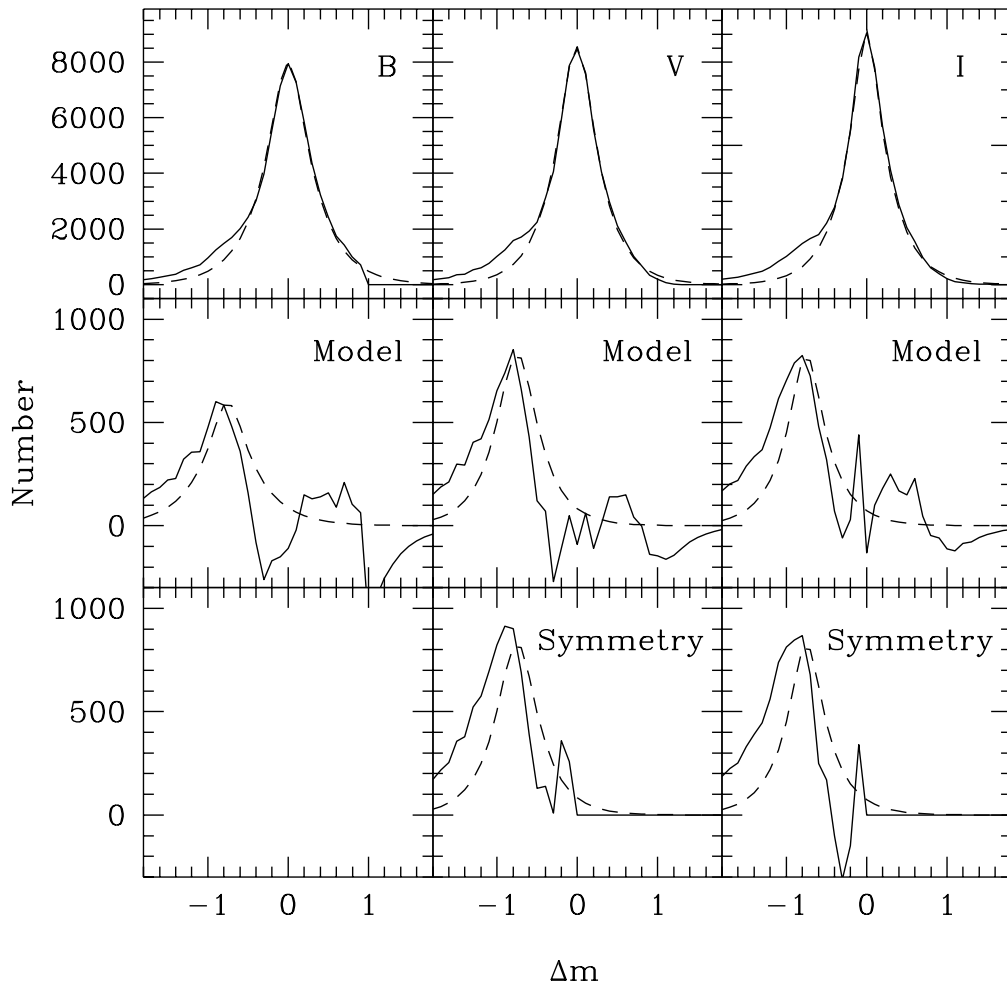


Fig. 5.—

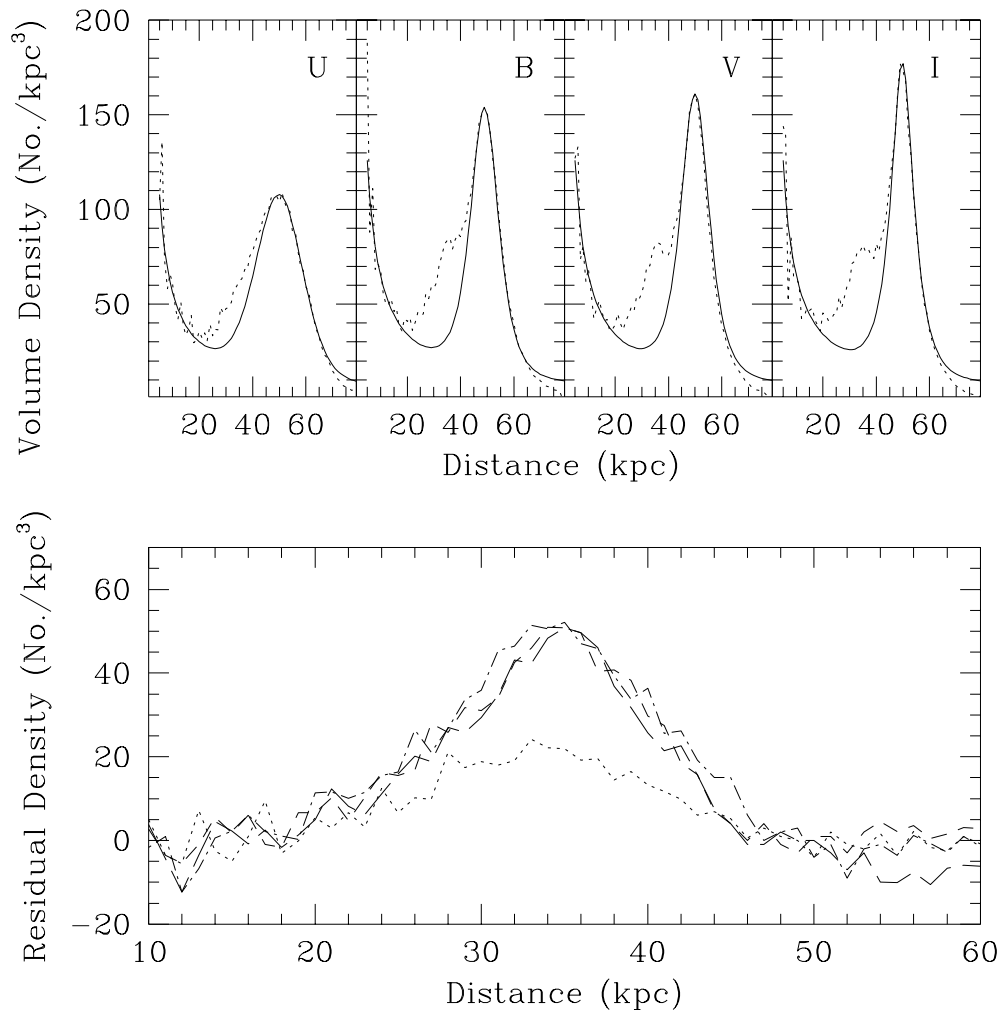


Fig. 6.—

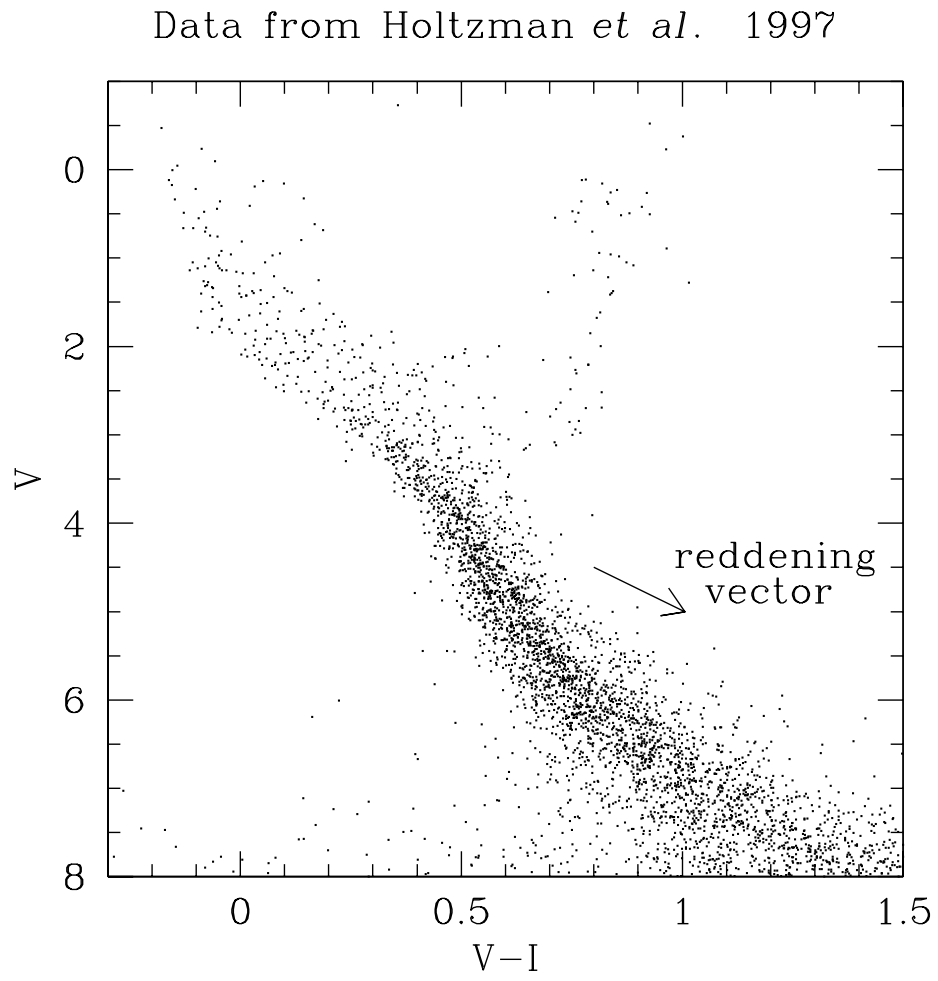


Fig. 7.—

